Proceedings of the ASME 2010 3rd Joint US-European Fluids Engineering Summer Meeting and 8th International Conference on Nanochannels, Microchannels, and Minichannels
FEDSM-ICNMM2010
August 1-5, 2010, Montreal, Canada

FEDSM-ICNMM2010-31249

NUMERICAL SIMULATION OF GAS-LIQUID TWO-PHASE FLOWS ON WETTED WALLS

Yoshiyuki Iso
IHI INC., Business Development Division
150 East 52nd Street, 24th Floor., New York, NY 10022, USA
E-mail : yoshiyuki_iso@ihi.co.jp

Xi Chen
Columbia University, Department of Earth and Environmental Engineering
500 West 120th Street, New York, NY 10027, USA
E-mail : xichen@columbia.edu

Keywords: gas-liquid two-phase flow, wetted wall flow, film, rivulet, transition, packed column, texture, CFD

ABSTRACT

Gas-liquid two-phase flows on the wall like liquid film flows, which are the so-called wetted wall flows, are observed in many industrial processes such as absorption, desorption, distillation and others. For the optimum design of packed columns widely used in those kind of processes, the accurate predictions of the details on the wetted wall flow behavior in packing elements are important, especially in order to enhance the mass transfer between the gas and liquid and to prevent flooding and channeling of the liquid flow.

The present study focused on the effects of the change of liquid flow rate and the wall surface texture treatments on the characteristics of wetted wall flows which have the drastic flow transition between the film flow and rivulet flow. In this paper, the three-dimensional gas-liquid two-phase flow simulation by using the volume of fluid (VOF) model is applied into wetted wall flows. Firstly, as one of new interesting findings in this paper, present results showed that the hysteresis of the flow transition between the film flow and rivulet flow arose against the increasing or decreasing stages of the liquid flow rate. It was supposed that this transition phenomenon depends on the history of flow pattern as the change of curvature of interphase surface which leads to the surface tension. Additionally, the applicability and accuracy of the present numerical simulation were validated by using the existing experimental and theoretical studies with smooth wall surface. Secondary, referring to the texture geometry used in an industrial packing element, the present simulations showed that surface texture treatments added on the wall can improve the prevention of liquid channeling and can increase the wetted area.

1. INTRODUCTION

Gas-liquid two-phase flows on walls like liquid film flows, which are called as wetted wall flows, are observed in many industrial processes such as absorption, desorption, distillation and others. Controlling these wetted wall flows efficiently is one of the key design factors for such devices, since they determine the process performances and limit of the operations. For the optimum design of packed columns widely used in those kind of processes, the accurate predictions of the details on the wetted wall flow behavior in packing elements are important, especially to enhance the mass transfer between the gas and liquid phases and to prevent flooding and channeling of the liquid flow.

As the fundamental researches, typical liquid falling film flows have been often studied theoretically and experimentally (Nusselt, 1916; Phan and Narain, 2007; Wang, 2009). However, it is still not easy to apply these results directly into the predictions in the specific industrial packed columns, because it is difficult to use them universally under the various conditions and it is risky to use them beyond the range of their assumption.

On the other hand, several experimental studies have been conducted for the specific packed columns in order to improve the mass transfer performance and to develop empirical modelings (Bravo et al., 1985 & 1995; Spiegel and Meier, 2003; Murrieta et al., 2004; Sidi-Boumedine and Raynal, 2005; Ataki et al., 2006; Chen et al., 2007; Raynal et al., 2009). In most cases, however, these experimental studies have been carried out by using air-water flows instead of the actual fluids and by using smaller or simpler experimental models than industrial ones. Thus, the fluid properties effects and scale effects on the hydrodynamics and mass transfer are not well known.

Recently, computational fluid dynamic (CFD) simulations are useful as an alternative to experiments, because multiphase flow measurements in the complex geometries such as packing elements are very difficult and highly expensive, especially at the industrial large scale with actual flow conditions. In the recent years, several studies can be found in the literature, which deal with the CFD simulations of gas-liquid two-phase flows in packed columns (Spiegel and Meier, 2003; Valluri et al., 2005; Ataki et al., 2006; Chen et al., 2007; Raynal et al., 2007 & 2009; Kenig, 2008; Ludwig and Dziak, 2009). In these studies, two-dimensional or three-dimensional CFD simulations have been used with the volume of fluid (VOF) model, which is a surface tracking technique in the Eulerian mesh. Several usable results have been achieved such as the liquid thickness, hold up, gas pressure drop, validation of CFD and so on.

Additionally, fewer studies exist on not only two-phase but also three-phase film flows on an inclined wall (Hoffmann et al., 2005 & 2006; Repke et al., 2007). Both the CFD and experiment have been carried out to predict the liquid film break-up, rivulet and droplet formation. Their studies have shown that this film break-up behavior has the three-dimensionality and is strongly influenced by the geometry.

Nevertheless, there is a lack of the literature data for the detailed descriptions of the various difficulties of the transition phenomena between the film flow and rivulet flow and effects of wall surface texture treatments on this kind of transition.

The present study focuses on the effects of the change of liquid flow rate and the wall surface texture treatments on the characteristics of wetted wall flows which have the drastic flow transition between the film flow and rivulet flow. Especially, this study investigates and discusses the details of this flow transition by adding new findings such as the hysteresis phenomena and those mechanisms, which have not been reported in existing literature. This study is important in order to prevent the channeling and flooding of liquid flow and to enhance the mass transfer performance.

In this paper, the three-dimensional gas-liquid two-phase flow simulation by using VOF model is applied into wetted wall flows. Firstly, the details of flow transition are investigated by increasing and decreasing the liquid flow rate. Additionally, the applicability and accuracy of the present numerical simulation are validated by using the existing experimental and theoretical studies with smooth wall surface. Secondary, the effects of wall surface texture treatments on the prevention of liquid channeling and increase of wetted area are investigated.

NOMENCLATURE

v	velocity [ms^{-1}]
t	time [s]
p	static pressure [Pa]
g	gravitational acceleration [ms^{-2}]
S	source term, S_m [Nm^{-3}] or S_f [$kgm^{-3}s^{-1}$]
f	volume fraction [-]
F	force [N]
V	representative velocity [ms^{-1}]
L	representative length [m]
Re	Reynolds number [-]
Fr	Froude number [-]
We	Weber number [-]
Q	volumetric flow rate [m^3s^{-1}]
w	width [m]
A	area [m^2]
a	amplitude of the surface texture [m]

Greek letters

α	inclined angle of the wall plate [degree]
ρ	density [kgm^{-3}]
μ	viscosity [Pas]
σ	surface tension coefficient [Nm^{-1}]
δ	liquid film thickness [m]
λ	length of the surface texture [m]

Subsripts

l	liquid phase
g	gas phase
m	momentum
k	phase k
f	volume fraction
i	inertia
v	viscosity
gr	gravity
st	surface tension
N	Nusselt theory
w	wetted surface
t	total surface of the plate

2. NUMERICAL METHOD

2.1 Computational Region and Flow Conditions

As the outline of the present flow objects, the computational region and a sample of grid for wetted wall flows are shown in **Figure 1**. Additionally, **Figure 2** shows two example images of typical wetted wall flows which are the full film flow and rivulet flow.

The geometry and flow conditions are set up in order to validate present simulations by using the existing studies for the wetted wall flows on the inclined wall plate (Hoffmann et al., 2005 & 2006; Repke et al., 2007). The inclined wall plate is the 0.06×0.05 m^2 stainless steel plate, a flow field length of 0.06m and width of 0.05m, which is held by supports on the left and on the right hand side of same stainless steel. The inclined angle of the wall plate α is 60 degree referring to the

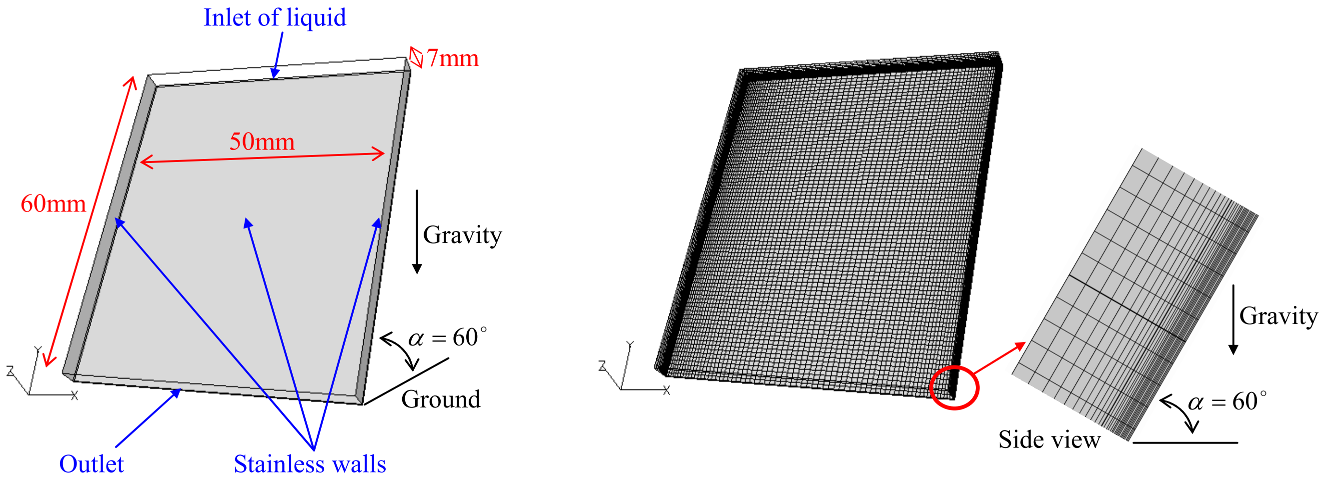

(a) Computational region (b) Computational grid

Figure 1: The computational region and a sample of grid for wetted wall flows

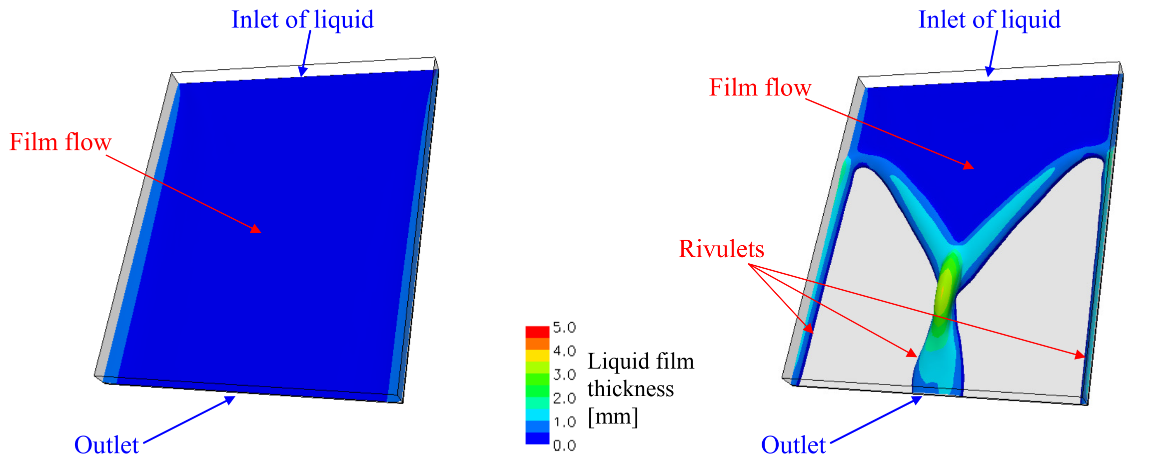

(a) Full film flow (b) Rivulet flow (Channeling flow)

Figure 2: Two images of typical wetted wall flows in the present case (Birds-eye view)

horizontal ground, which is the inclination used commonly for the commercial structured packing.

As the gas-liquid two-phase fluids, the well known air-water is used. The physical properties of gas and liquid implemented in this simulation are referred to the existing experiment (Hoffmann et al., 2006). As the physical properties of gas, density ρ_g is 1.185 kg/m^3, viscosity μ_g is 1.831×10^{-5} Pa$\cdot$s. As the physical properties of liquid, density ρ_l is 997 kg/m^3, viscosity μ_l is 8.899×10^{-4} Pa$\cdot$s, surface tension coefficient σ_l is 0.0728 N/m. The static contact angle for air and water on the stainless steel is applied 70 degree obtained by the experimental measurement (Hoffmann et al., 2005 & 2006).

The liquid inlet condition is assumed as a uniform film flow to consider the experimental liquid feeding conditions using an overflowing weir in order to make the formation of a stable film flow. The plate and both side supports are implemented as no-slip walls with given contact angles. The other boundaries, which are upward, downward outlet and top boundaries, are set to the pressure outlet conditions by using defined static pressures.

Additionally, the computational grid is made very fine for sufficiently accurate resolution of the liquid flow, since several test cases were performed to validate the grid convergence.

2.2 CFD Modeling for Gas-Liquid Two-Phase Flows

In this study, CFD simulations are carried out with the commercial code FLUENT, ANSYS Inc. The three-dimensional and transient model for gas-liquid two-phase flow simulations by a volume of fluid (VOF) model are used to predict the wetted wall flows, because the existing studies have shown that rivulet flows are influenced strongly by three dimensional effects and therefore cannot be predicted by analytical approaches and two-dimensional CFD simulations (Hoffmann et al., 2005 & 2006; Ataki et al., 2006; Repke et al., 2007).

The CFD models are based on the universal transport equations of extensive magnitudes in differential volume of the fluid. In case of hydrodynamics modeling, two conservation equations of the mass and momentum are solved numerically. The mass conservation leads to the continuity equation, and the momentum conservation gives the Navier-Stokes equation, as follows:

$$\frac{\partial \rho}{\partial t} + \nabla \cdot (\rho \cdot \boldsymbol{v}) = 0 \tag{1}$$

$$\frac{\partial (\rho \cdot \boldsymbol{v})}{\partial t} + \nabla \cdot (\rho \boldsymbol{v} \cdot \boldsymbol{v}) = -\nabla p + \nabla \cdot \left[\mu \left(\nabla \boldsymbol{v} + \nabla \boldsymbol{v}^{\mathrm{T}} \right) \right] + \rho \boldsymbol{g} + \boldsymbol{S}_m \tag{2}$$

where $\boldsymbol{v}$ and p are the velocity vector and static pressure of the fluid, respectively. $\boldsymbol{S}_m$ is the source term vector expressing the momentum sources such as the surface tensions, the external forces and so on.

In this study, the set of these two equations is applied into the single field shared among all phases, which is called the shared-field approach, by using the Eulerian method. In this case, turbulence is not taken into account since the range of the Reynolds number of liquid flow indicates laminar.

Additionally, using the VOF model, the interphase surface tracking technique is applied into the fixed Eulerian mesh. The set of the above mass and momentum equations can be accomplished with the relation describing the interphase surface position. This relation is described by:

$$\frac{\partial (\rho_k f_k)}{\partial t} + \nabla \cdot (\rho_k f_k \cdot \boldsymbol{v}_k) = S_{f\,k} \tag{3}$$

where f_k and $\boldsymbol{v}_k$ are the volume fraction and velocity vector of the phase k, respectively. S_f is the source term expressing the mass sources such as the mass transfer between phases, supplied mass and so on. In this case, S_f is zero on the assumption that the mass transfer between gas and liquid can be negligible.

In this VOF model, these volume fractions are assumed to be continuous functions of space and time, and the sum of volume fractions is equal to one. If $f_k = 0$, the calculation cell is empty of the phase k. When $f_k = 1$, the calculation cell is filled with the phase k. For $0 < f_k < 1$, the calculation cell contains the interphase surface between the phase k and one or more other phases.

As above mentioned, the set of the mass and momentum equations, which is shared in the single field among the all phases, is dependent on the volume fractions of all phases through the local fluid properties such as the density, viscosity and so on. The local fluid properties in the calculation cell are calculated by using a linear interpolation as the volume fraction average.

The effects of surface tensions along the interface between each pair of phases are implemented with the continuous surface force (CSF) model proposed by Brackbill et al. (1992). The surface tension can be considered in terms of the pressure jump across the interphase surface. In this CSF model, the addition of surface tension to the VOF model results in a source term $\boldsymbol{S}_m$ in the momentum equation.

Additionally, in order to consider the effects of wall adhesion, contact angles between the phases and walls are imposed as wall boundary condition. The wall adhesion model proposed by Brackbill et al. (1992) is used. The contact angles derived from static data are implemented by setting the angle of the gradient of the volume fraction at the wall boundary condition. The local curvature of the interphase surface in the calculation cell next to the wall is used to adjust the body force term in the surface tension calculation.

3 CHARACTERIZATIONS OF WETTED WALL FLOWS

3.1 Dominant Forces on Liquid Flows

In this section, the dimensionless groups which characterize the present liquid flow are derived by considering the forces. In the case of the present wetted wall flows, it is generally accepted that the dominant forces on the liquid flow characteristics are four forces: inertia force F_{li}, viscous force F_{lv}, gravitational force F_{lgr} and surface tension F_{lst}. Using the representative velocity V_l and length L_l related to the outline system of this liquid flow, the above forces are defined as follows:

$$F_{li} \approx \rho_l V_l^2 L_l^2 \tag{4}$$

$$F_{lv} \approx \mu_l V_l L_l \tag{5}$$

$$F_{lgr} \approx (\rho_l - \rho_g) g L_l^3 \tag{6}$$

$$F_{lst} \approx \sigma L_l \tag{7}$$

Normalizing the dominant forces by the inertia force, the dimensionless groups can be obtained by the following:

$$\frac{F_{lv}}{F_{li}} = \frac{\mu_l V_l L_l}{\rho_l V_l^2 L_l^2} = \frac{\mu_l}{\rho_l V_l L_l} = \frac{1}{\mathrm{Re}_l} \tag{8}$$

$$\frac{F_{lgr}}{F_{li}} = \frac{(\rho_l - \rho_g) g L_l^3}{\rho_l V_l^2 L_l^2} = \frac{(\rho_l - \rho_g) g L_l}{\rho_l V_l^2} \approx \frac{g L_l}{V_l^2} = \frac{1}{\mathrm{Fr}_l} \tag{9}$$

$$\frac{F_{lst}}{F_{li}} = \frac{\sigma L_l}{\rho_l V_l^2 L_l^2} = \frac{\sigma}{\rho_l V_l^2 L_l} = \frac{1}{\mathrm{We}_l} \tag{10}$$

The dimensionless groups which characterize the present liquid flow can be written by the above equations, namely:

$$\mathrm{Re}_l = \frac{\rho_l \cdot V_l \cdot L_l}{\mu_l} \tag{11}$$

$$\mathrm{Fr}_l = \frac{V_l^2}{g \cdot L_l} \tag{12}$$

$$\mathrm{We}_l = \frac{\rho_l \cdot V_l^2 \cdot L_l}{\sigma} \tag{13}$$

3.2 Definition of Dimensionless Groups

In this section, the dimensionless groups are redefined by using the suitable representative quantities in order to apply it into the present wetted wall flows. It starts to consider the traditional expression of the falling film thickness introduced by Nusselt (1916). This expression is the well known Nusselt theory, in which the balance of only two forces between gravitational force and friction force on a fluid element in the film is considered by assuming the steady continuous liquid film flow to be formed uniformly on the plate. Using these classical works of Nusselt theory, both falling film thickness and velocity distribution can be calculated.

In the case of the falling liquid film flow on the inclined plate, the liquid film thickness δ_{N} is expressed as follows:

$$\delta_{\mathrm{N}} = \left[\frac{3\mu_l \cdot Q_l}{(\rho_l - \rho_g) \cdot g \sin\alpha \cdot w} \right]^{1/3} \tag{14}$$

where Q_l is the volumetric flow rate of liquid. w is width of the liquid film on the plate, which is assumed to be equal to the plate width as full film flow developing completely on the whole plate area in this case.

Using the liquid film thickness δ_{N} obtained by the Nusselt theory, the above derived dimensionless groups are redefined, which can be applied into the present wetted wall flows, namely:

$$\mathrm{Re}_{l\mathrm{N}} = \frac{\rho_l \cdot V_{l\mathrm{N}} \cdot \delta_{\mathrm{N}}}{\mu_l} \tag{15}$$

$$\mathrm{Fr}_{l\mathrm{N}} = \frac{V_{l\mathrm{N}}^2}{g \cdot \delta_{\mathrm{N}}} \tag{16}$$

$$\mathrm{We}_{l\mathrm{N}} = \frac{\rho_l \cdot V_{l\mathrm{N}}^2 \cdot \delta_{\mathrm{N}}}{\sigma} \tag{17}$$

where $V_{l\mathrm{N}}$ is the averaged liquid film velocity defined by the following:

$$V_{l\mathrm{N}} = \frac{Q_l}{\delta_{\mathrm{N}} \cdot w} \tag{18}$$

In this study, after-mentioned several present results are explained relating to these dimensionless groups. Especially, the Weber number $\mathrm{We}_{l\mathrm{N}}$ is used for considering the balance between inertia force and surface tension, which is an important parameter for the flow transition phenomenon.

4. RESULTS AND DISCUSSION

The present paper investigated and discussed the effects of the change of liquid flow rate and the wall surface texture treatments on the characteristics of wetted wall flows which have the drastic flow transition between the film flow and rivulet flow.

4.1 Wetted Wall Flows on the Smooth Surface

In this section, the effects of the change of liquid flow rate on the flow transition of wetted wall flows on the smooth surface are investigated. Additionally, the applicability and accuracy of the present numerical simulation are validated by using the existing experimental and theoretical studies (Nusselt, 1916; Hoffmann et al., 2005 & 2006; Repke et al., 2007).

Figure 3 shows that the wetted areas A_w/A_t obtained by present simulations are plotted over the Weber number $\mathrm{We}_{l\mathrm{N}}$ with the existing experimental data. Additionally, the interphase surfaces between gas and liquid obtained by the present simulations are shown in **Figure 4**. The interphase surfaces between gas and liquid are visualized using the iso-surfaces which are defined by the specific volume fraction of liquid. As can be seen in **Figure 4**, two types of flow patterns are observed in this case. First type is the full film flow, which means film flow is only formed on the whole plate. Second type is the channeling flow, which means both of the film flow and rivulet flows are formed on the plate.

Firstly, as one of new interesting findings in this paper, the present results show that the transition patterns between the full film flow and rivulet flow, where the wetted area changes between A_w/A_t =1 and less, are different significantly against the increasing or decreasing stages of the Weber number. Additionally, this difference of transition shows clearly that there is the hysteresis phenomenon in the transition region. While the liquid flow rate is increasing which means the Weber number is increasing, the wetted area is increasing continuously from the rivulet flow to the full film flow. While the liquid flow rate is decreasing which means the Weber number is decreasing, however, the wetted area decreases suddenly from the full film flow to the rivulet flow at the lower critical Weber number than one while the liquid flow rate is increasing.

It is supposed that the main reason, why the above hysteresis occurs, is the surface tension depends strongly on the curvature of the interphase surface between gas and liquid. When the film flow is formed continuously, the curvature of the interphase surface is almost zero, and then the surface tension on the liquid film surface is very low. On the other hand, when the rivulet flows are formed once, the surface tension forces strongly on the rivulet surface because the rivulet has the curvature of the interphase surface. Thus, it should be denoted that this flow transition between the film flow and rivulet flow depends on the history of flow pattern as the change of curvature of interphase surface which leads to the surface tension.

Here, the liquid flow rate is changed as step-like pattern not continuously in this simulation. Under each liquid flow rate, each simulation result is obtained as the quasi-steady convergent solution by using the previous solution at the nearest liquid flow rate as the initial condition. However, the hysteresis pattern observed in this paper might depend on the variation of the change of liquid flow rate. That is another interesting point of this study in the future.

Secondary, as the validation of the present simulation, the critical range of the flow transition between the film flow and rivulet flow can be accurately predicted by comparing between the present simulation results and the experimental results in **Figure 3**. Additionally, in terms of the liquid flow shape, the

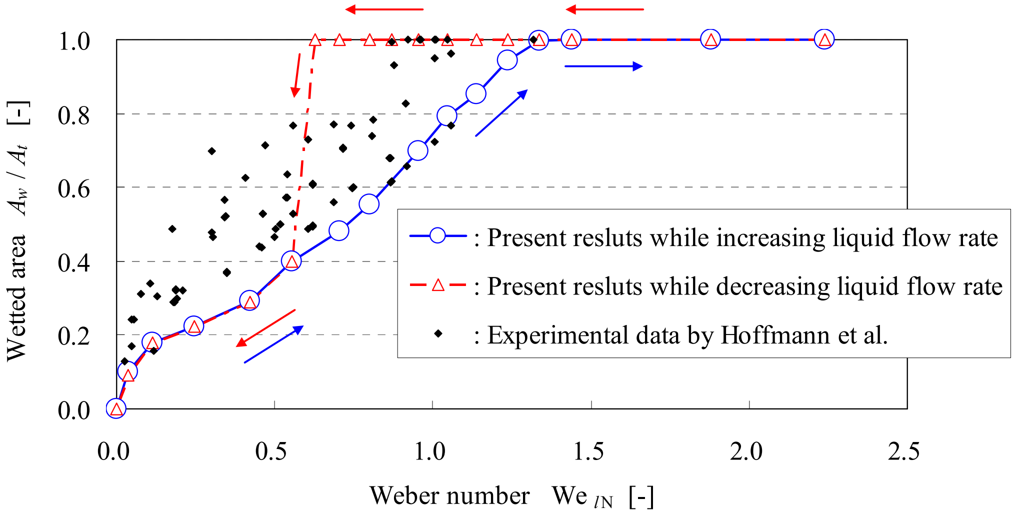

Figure 3: The wetted areas A_w/A_t as a function of the Weber number $\mathrm{We}_{l\mathrm{N}}$

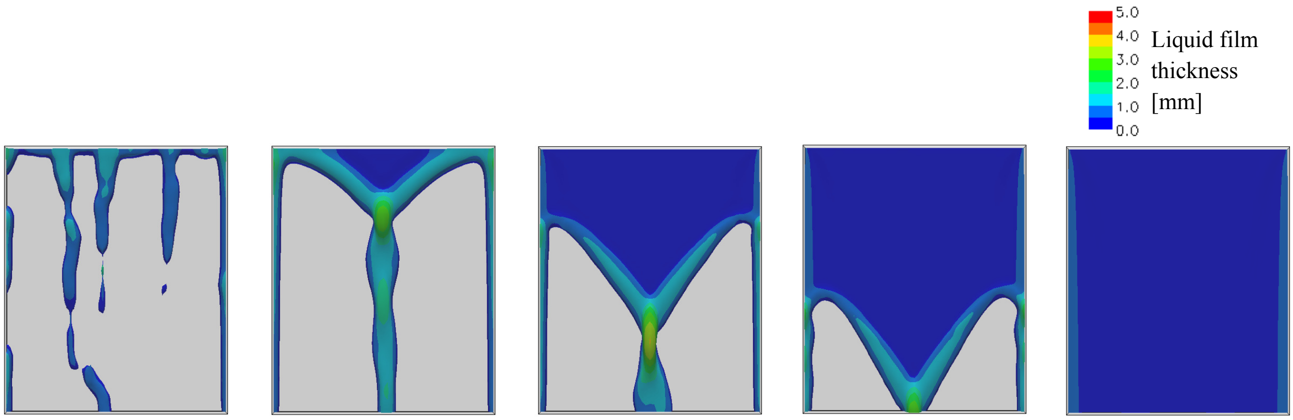

Channeling flow (a) $\mathrm{We}_{l\mathrm{N}}$ =0.04 | Channeling flow (b) $\mathrm{We}_{l\mathrm{N}}$ =0.42 | Channeling flow (c) $\mathrm{We}_{l\mathrm{N}}$ =0.80 | Channeling flow (d) $\mathrm{We}_{l\mathrm{N}}$ =1.05 | Full film flow (e) $\mathrm{We}_{l\mathrm{N}}$ =1.44

Figure 4: The comparison of liquid flow patterns visualized by interphase surfaces between gas and liquid (While the liquid flow rate is increasing)

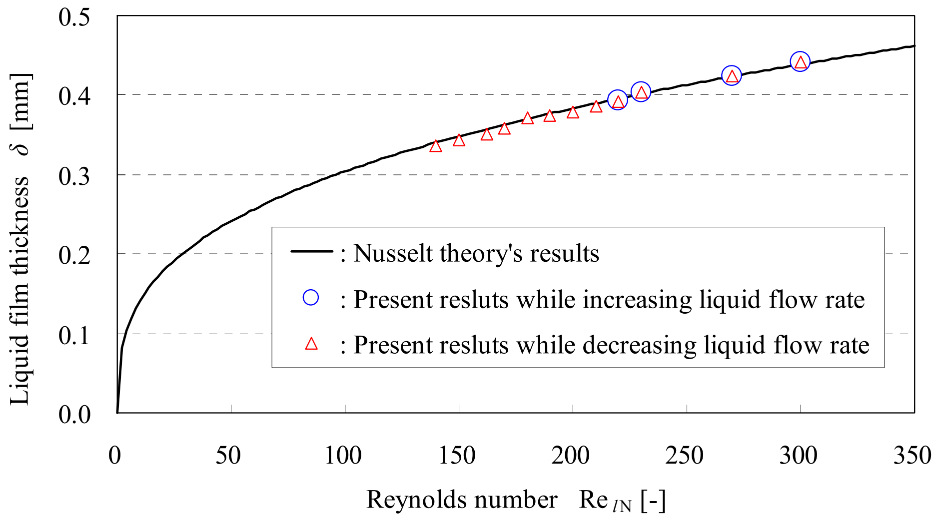

Figure 5: The liquid film thickness δ as a function of the Reynolds number $\mathrm{Re}_{l\mathrm{N}}$ (Stable film flows are formed, when A_w/A_t=1)

present simulation results show very good agreement qualitatively with the experimental photos obtained by Hoffmann et al. (2006).

Another validation is conducted about the liquid film thickness δ. The simulation results of liquid film thickness in the range in which full film flows are formed, when A_w/A_t =1, are compared to the above mentioned Nusselt theory (Nusselt, 1916). The comparison data between the present simulations and Nusselt theory's results are plotted over Reynolds number $\mathrm{Re}_{l\mathrm{N}}$ in **Figure 5**. The present simulation results are calculated at the center location in the flow width after the full film flow is developed completely. **Figure 5** shows a good agreement between the present simulations and Nusselt theory's results. When the full film flow is formed, Reynolds number is the better parameter to characterize the film flow behavior than Weber number, since the surface tension on the film flow is very low. In other words, it can be mentioned that the hysteresis phenomenon cannot be seen in this range, because the surface tension is not important for the full film flow.

These validations show that the present two-phase flow simulation by using VOF model is capable of predicting the flow transition of wetted wall flows between the film flow and rivulet flow on the inclined smooth wall.

4.2 Effects of Wall Surface Texture Treatments

It can be found that the several industrial packing elements have the wall surface treatments such as small texture or perforations in order to prevent the liquid channeling as the film break-up and to increase the wetted area (Valluri et al., 2005; Ataki et al., 2006; Raynal et al., 2007 & 2009). In this section, the effects of wall surface texture treatments on the flow transition of wetted wall flows are investigated.

Figure 6 shows the outline of the small surface texture on the inclined wall used in the present simulation. The amplitude a and length λ of the surface texture are selected referring to an industrial packing element (Raynal et al., 2007 & 2009). In this case, the amplitude of the surface texture is the same order as the liquid film thickness.

An example of results obtained the present simulations is shown in **Figure 7**. These two results are simulated under the same flow conditions ($\mathrm{We}_{l\mathrm{N}}$ =1.14). The channeling flow occurs in the case of the smooth surface wall. The full film flow, however, is kept on the whole plate in the case of the small texture treatments added on the wall surface. In this flow condition, the wall surface texture treatments give the approximately 1.17 times larger wetted area than one on the smooth wall.

Thus, the present results show that surface texture treatments added on the wall can improve the prevention of liquid channeling and can increase the wetted area.

5. CONCLUSIONS

The present study was carried out to investigate the effects of the change of liquid flow rate and the wall surface texture treatments on the characteristics of wetted wall flows.

Firstly, present results showed that the hysteresis of flow transition between the film flow and rivulet flow arose against the increasing or decreasing stages of the liquid flow rate which means the Weber number is changing. It should be denoted that this transition phenomenon depends on the history of flow

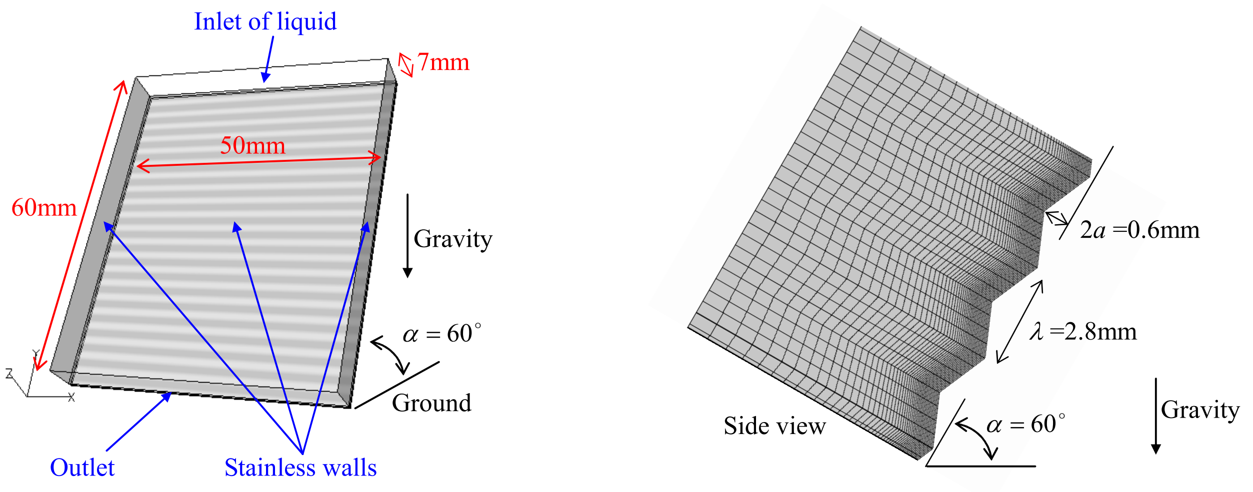

(a) Computational region with wall surface texture (b) Details of the wall surface texture (Zoom of computational grid)

Figure 6: The computational region and a sample grid for wetted wall flows with wall surface texture treatments

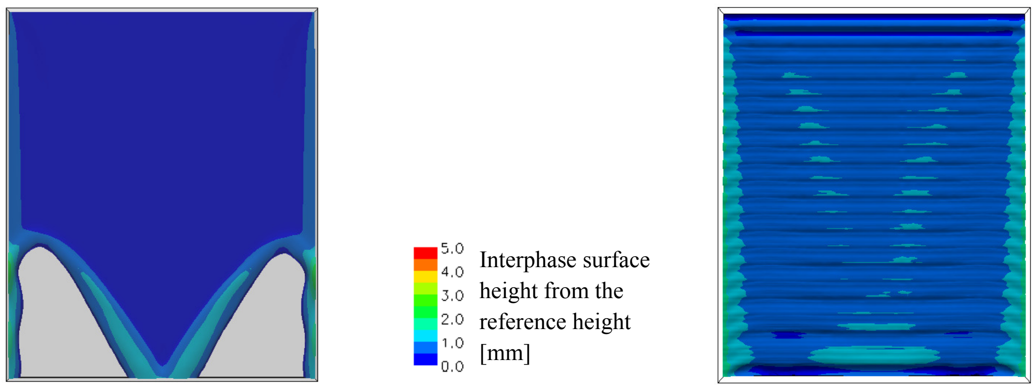

(a) The result on the smooth surface wall (We_{lN} =1.14) (b) The result on the wall with surface texture (We_{lN} =1.14)

Figure 7: The comparison of liquid flow patterns visualized by interphase surfaces between gas and liquid (While the liquid flow rate is increasing)

pattern as the change of curvature of interphase surface which leads to the surface tension. Additionally, the applicability and accuracy of the present numerical simulation were validated by using the existing experimental and theoretical studies for the wetted wall flows on the smooth surface.

Secondary, referring to the texture geometry used in an industrial packing element, the present results show that surface texture treatments added on the wall can improve the prevention of liquid channeling and can increase the wetted area.

As the results, present study showed that this numerical simulation by using VOF model can be applied into not only the investigation of wetted wall flow behavior such as film break-up and rivulet flow but also the optimization of the design of packing elements.

In the future, a next step will be to investigate the effect of wall surface texture more systematically. Furthermore, another next step will be to investigate more complex geometries and flow conditions such as industrial large scale packing with actual flow conditions, and to develop a better designing method for those two-phase flow processes.

ACKNOWLEDGMENTS

The authors would like to appreciate gratefully the fruitful conversation and support by our colleagues in the Professor

Chen's research group at the Columbia University. Additional support was received from IHI Corporation.

REFERENCES

Ataki, A., Kolb, P., Buhlman, U. and Bart, H. J., Wetting performance and pressure drop of structured packings: CFD and experiment, IChemE, Symposium Series, 152, pp. 534-543 (2006)

Ataki, A., and Bart, H. J., Experimental and CFD simulation study for the wetting of structured packing element with liquid, Chemical Eng. and Tech., 29, 3, pp. 336-347 (2006).

Brackbill, J. U., Kothe, D. B. and Zemach, C., A continuum method for modeling surface tension, J. of Comp. Physics, 100, pp. 335-354 (1992).

Bravo, J. L., Rocha, J. A. and Fair, J. R., Mass transfer in gauze packings, Hydrocarbon Processing, 64, 1, pp. 91-95 (1985).

Bravo, J. L., Rocha, J. A. and Fair, J. R., A comprehensive model for the performance of columns containing structured packings, Inst. Chem. Eng. Symp. Series, 128, pp. A439-A457 (1992).

Chen, J., Liu, C., Li, Y., Huang, Y., Yuan, X. and Yu, G., Experimental investigation of single-phase flow in structured packing by LDV, Chin. J. Chem. Eng., 15, 6, pp. 821-827 (2007).

Hoffmann, A., Ausner, I., Repke, J. U. and Wozny, G., Fluid dynamics in multiphase distillation processes in packed towers, Computers and Chemical Eng., 29, pp. 1433-1437 (2005).

Hoffmann, A., Ausner, I., Repke, J. U. and Wozny, G., Detailed investigation of multiphase flow behaviour on inclined plates, Trans. IChemE, Chemical Eng. Research and Design, 84, A2, pp. 147-154 (2006).

Kenig, E. Y., Complementary modeling of fluid separation processes, Chemical Engineering Research and Design, 86, pp. 1059-1072 (2008).

Ludwig, W. and Dziak, J., CFD modelling of a laminar film flow, Chemical and Process Eng., 30, pp. 417-430 (2009).

Murrieta, C. R., Sebert, A. F., Fair, J. R. and Rocha-U, J. A., Liquid-side mass-transfer resistance of structured packings, Ind. Eng. Chem. Res., 43, pp. 7113-7120 (2004).

Nusselt, W., Die oberflachenkondensation des wasserdampfes, Zeitschr. Ver. Deut. Ing., 60, pp. 541-546 and pp. 569-575 (1916).

Phan, L. and Narain, A., Nonlinear stability of the classical Nusselt problem of film condensation and wave effects, Trans. of the ASME, J. of Applied Mechanics, 74, pp. 279-290 (2007).

Raynal, L. and Royon-Lebeaud, A., A multi-scale approach for CFD calculations of gas-liquid flow within large size column equipped with structured packing, Chemical Eng. Science, 62, pp. 7196-7204 (2007).

Raynal, L., Rayana, F. B. and Royon-Lebeaud, A., Use of CFD for CO_2 absorbers optimum design: from local scale to large industrial scale, Energy Procedia, 1, pp. 917-924 (2009).

Repke, J. U., Ausner, I., Paschke, S. Hoffmann, A. and Wozny, G., On the track to understanding three phases in one tower, Trans. IChemE, Chemical Eng. Research and Design, 85, A1, pp. 50-58 (2007).

Sidi-Boumedine, R. and Raynal, L., Influence of the viscosity on the liquid hold-up in trickle-bed reactors with structured packings, Catalysis Today, 105, pp. 673–679 (2005).

Spiegel, L. and Meier, W., Distillation columns with structured packings in the next decade, Trans. IChemE, 81, Part A, pp. 39-47 (2003).

Valluri, P., Matar, O. K., Hewitt, G. F. And Mendes, M. A., Thin film flow over structured packings at moderate Reynolds numbers, Chemical Eng. Science, 60, pp. 1965-1975 (2005).

Wang, X., He, M., Fan, H. and Zhang, Y., Measurement of falling film thickness around a horizontal tube using laser-induced fluorescence technique, J. of Physics, Conf. Series, 147, 012039 (2009)

